

Karst flash flood in a Mediterranean karst, the case of Fontaine de Nîmes

JC. Maréchal (✉), B. Ladouche and N. Dörfliger

BRGM, Water Department, 1039 rue de Pinville, 34 000 Montpellier, France¹

Abstract

Karst flash flooding, identified as one of the hazards in karst terrains, is directly linked to the structure and hydraulic properties of karst aquifers. Due to the characteristics of flow within karst aquifers, characterized by a dual flow – diffuse flow within fissured limestone and conduit flow within karst conduits networks – flash flooding may be important in volume and dynamics. Such phenomenon may cause serious damages including loss of lives, as it occurred on 3rd October 1988 in Nîmes (Gard, South France). Flash floods there have been considered to be the result of very intensive rainfall events conjugated to runoff due to the geomorphologic context of the city located down hill. However, preliminary results of recent studies of the hydrologic behaviour of groundwater and surface water for a specific event (September 2005) based on an extensive monitoring of the karst aquifer coupled to a classical runoff monitoring show that the role of the karst in the flood genesis plays an important role. The main characteristics of the Nîmes karst system leading to karst flash flooding are presented in this paper. A methodology comprising modelling of the karst system allowed proposing simple thresholds for various part of the karst (water level threshold for the karst conduits and cumulative rainfall threshold for the overflowing fissured karst). These thresholds can be included in the flash flood warning system of the Nîmes city.

Keywords

Flash-Flood, Groundwater, Hazard, Karst, Spring, Water Table

1. Introduction

Four main geologic hazards are generally associated with karst: cover-collapse sinkholes (Kaufmann and Quinif, 1999), sinkhole flooding (Lolcama et al., 2002), high concentrations of radon in basements and crawl spaces of houses (O'Connor et al., 1993) and groundwater vulnerability (Andreo et al., 2006). Recently, karst flash flooding has been identified as a new kind of hazard in karst terrains (Bonacci et al., 2006). A flash flood is defined as a flood which follows shortly (i.e. within a few hours) after a heavy or excessive rainfall event (Georgakakos, 1986).

Karst aquifers are characterized by a dual flow system (Király, 1994) consisting of a fissured system which represents the bulk mass of limestone storing water with Darcyan flow, and a conduit system with the karst conduit network transmitting water by turbulent flows (Atkinson, 1977). Exchange between the two systems is controlled by

¹ Fax: + 33 4 67 15 79 75, jc.marechal@brgm.fr; b.ladouche@brgm.fr; n.dorfliger@brgm.fr

hydraulic head differences as well by the hydraulic conductivities and the geometric setting (Atkinson, 1977).

Due to the characteristics of groundwater circulation in karst terrains, flash flooding in such context is strongly different than in non karst terrains, the volume of water during a karst flash flood being much more important than in cases of non-karst flash floods. The main cause is the rapid circulation of large quantities of infiltrated water through karst conduits with a dynamic very close to surface water runoff.

The Nîmes city has been forever subject to catastrophic floods events. History of the city mentions about 42 flood events from 1334 to 2005, about one flood every 16 years as an average. Almost 60 % of the events happen during the three months between September and November. In the recent past, the most important one occurred on 3 October 1988 and killed 9 people among 45000 disaster victims (Fabre, 1990). Damages were about 600×10^6 euros. The specific maximum outflow discharge (q_M) of the Cadereaux rivers, defined as $q_M = Q_M / A$, where A is the catchment area (42 km^2) and Q_M is maximum estimated discharge ($1600 \text{ m}^3 \text{ s}^{-1}$ in 1988), is equal to $38.1 \text{ m}^3 \text{ s}^{-1} \text{ km}^{-2}$, the highest in a comparative study done by Stanescu and Matreata (1997) on flash floods along rivers in five European countries. These flash floods have been for a long time considered to be the result of very intensive rainfall events from Cevennes climate influence conjugated with the geomorphologic context (Ballais et al., 2005) of the city which is located at the bottom of a hill. Usually, overland flow tends to play the dominant role in flash flood formation and low infiltration capacity is the most important factor for overland flow development (Smith and Ward, 1998). However, with a very scarce and thin soil cover of high infiltration capacity, karstified limestone of Nîmes hills are in theory favourable to the infiltration of a part of rainwater, reducing the potential overland flow genesis. Therefore, soils characteristics in the watershed are such that flash flood should not happen in Nîmes city.

An extensive monitoring of the karst system has been coupled to the classical runoff monitoring during a recent event which occurred in September 2005. The preliminary results show that the role of the karst system in the flood genesis is very important and that the flash floods at Nîmes can be related to a phenomenon of karst flash flooding. This paper presents the main characteristics of the Nîmes karst leading to karst flash flooding.

2. Study area

The Fontaine de Nîmes (FdN) spring is located in the South-Eastern France, in the city of Nîmes. Most of the time, it constitutes the only discharge point of a karst system which is famous for its rapid reaction to rainfall events. The unsaturated zone is maximum ten meters thick and the saturated zone is limited to a few tens of meters. A well developed karstic network drains the aquifer to the FdN spring (Figure 1). A part of these drains has been mapped by speleologists during several diving explorations. Except for two publications (Fabre and Guyot, 1984; Fabre and Guyot, 1988), the hydraulics of the system is poorly known.

The area receives around 740 mm annual precipitation that recharges the karst aquifer mainly by diffuse infiltration and swallow holes. The springs of the system consist of the FdN spring, with a discharge comprised between 0.01 and 18 m³ s⁻¹, and several intermittent springs discharging only during flash floods.

The karst basin (Figure 1), defined by numerous tracing experiments (Fabre, 1997) and a water budget calculation (Maréchal et al., 2005; Pinault, 2001), is estimated to be on the order of 55 km². The area is quite a lot urbanised in the southern part and covered by natural Mediterranean vegetation (Garrigues) in the north. The catchment area is mainly composed of limestone from Hauterivian, Cretaceous.

The city is at the bottom of the hill at the convergence of three temporary streams called “cadereaux”, which is a local term designating the small valleys around Nîmes traversed very temporarily by torrential flows during rainy events: the Uzes stream from the east, the Ales stream from the north and the Camplanier stream from the west. These streams are monitored for their discharge by the City services in order to organise the alert and manage the emergency services during flood crisis.

A complementary observation network has been set-up at boreholes in order to monitor the water table fluctuation after rainy events and at the FdN spring for discharge monitoring (Figure 1).

Figure 1 : Location of the Eastern part of Nîmes karst system and Nîmes city area. Location of complementary monitoring network.

3. Results and analysis

3.1. Dynamics of the karst system

The rainy event of September 2005 occurred after a very long dry period. It was composed of two events (Figure 2a):

- 6th September 2005: a total rainfall of 150 mm to 250 mm mainly occurred between 13:30 and 18:30 with a maximum intensity ranging from 50 to 75 mm/hour (return period for that intensity is more than two years - Figure 2b);
- 8th September 2005: a total rainfall of 105 mm to 255 mm mainly occurred between 11:30 and 23:30 with a maximum intensity ranging from 30 to 50 mm/hour.

The geographical variability of the event was high with a total amount of rainfall varying between 260 and 500 mm according to the location. Figure 2a illustrates the cumulative amount of rainfall for this event according to its duration up to 72 hours and compares to the recent events in Nîmes (October 1988, May 1998 and September 2002).

Figure 2 : (a) Cumulative rainfall according to duration of the last main rainfall events at Nîmes (after Raymond et al., 2006); (b) Return period of rainfall of one hour duration at Nîmes Courbessac meteorological station

During the event, the discharge can be compared at the main spring of the karst system with an intermittent surface stream at a point located a few hundred meters upstream (Figure 3). Before the event, the surface stream was dry as it is the case most of the hydrological year and the discharge flow at the spring was very low (0.01 m³ s⁻¹). The first rainy event induced a higher discharge at the spring (15 m³ s⁻¹) than the moderate

runoff ($< 10 \text{ m}^3 \text{ s}^{-1}$) in the stream. The discharge peak arrived later at the spring but the time lag between both peaks was only two hours. The time lag between rainfall peak and discharge peak at the spring was only 7 hours: the groundwater flow through karst conduits is very fast. The second event, with about the same rainfall volume, induced a much higher discharge peak in the stream ($Q_M \approx 60 \text{ m}^3 \text{ s}^{-1}$; $q_M \approx 6 \text{ m}^3 \text{ s}^{-1} \text{ km}^{-2}$) than at the spring ($Q_M \approx 18 \text{ m}^3 \text{ s}^{-1}$). In the stream, the runoff coefficient of the second event (about 100 %) was much higher than for the first event (about 15 %). This suggests that a large part of the first event rainfall (85% of 230 mm, about 200 mm) has infiltrated and has been stored in the soils and/or karst. Retention capacities due to storage by infiltration from 100 to 250 mm have been reported during similar flash flood events of the Aude River in 1999 (Gaume et al., 2004). During the second event, the double reservoir constituted by soils and karst being saturated, the quantity of runoff increased a lot and created the large flood with a runoff coefficient close to 100 %. This is not a purely Hortonian runoff but an infiltration excess runoff.

It is remarkable that the dynamics of the karst response is very fast, almost simultaneous with the surface water peak. This is due to (i) rapid infiltration of storm flow entering the aquifer quickly through sinkhole drains and fissures and (ii) rapid circulation in flooded karstic conduits network. Therefore the peak of groundwater from the spring is added to the peak of surface water in the streams: this constitutes a second reason for the flood genesis in the city.

Figure 3 : Discharge rate of the main spring of the karst system (FdN spring) and in the Ales stream during September 2005 event

3.2. Limited capacity of the main karst spring: backflooding and sinkhole flooding

The exam of the sorted discharge rates diagram of the FdN spring on a long period (1998-2005) shows that during high flood periods ($Q > 13 \text{ m}^3 \text{ s}^{-1}$), the slope of straight line α_3 is superior to α_2 (Figure 4). When discharge exceeds $13 \text{ m}^3 \text{ s}^{-1}$, hydraulic properties of the hydrosystem change (slope break): the discharge rate at the main spring increases less quickly. This is typical of the participation of intermittent overflow springs to the total discharge of the system: therefore, the discharge at the main spring increases less because water is flowing elsewhere.

Figure 4 : Sorted discharge rates of FdN spring during 1998-2005 period ($0.05 \text{ m}^3 \text{ s}^{-1}$ class)

Some of these intermittent springs are very close to the known conduits network with which they are directly connected. An example (Figure 5) is a Roman well and a sinkhole which are flooding with significant discharge rates (as an example, $1.4 \text{ m}^3 \text{ s}^{-1}$ on 7th September and $2.2 \text{ m}^3 \text{ s}^{-1}$ on 9th September; Jouanen, Personal Communication). This flooding should be due to backup of excess flow behind a constriction in the major conduit leading to the spring: this phenomenon is known in karst hydrology as backflooding (Lowe and Waltham, 2002). Indicators of flow inversion (diving rope displacement) have been observed by speleologist divers in the conduit after large floods (Jouanen, Personal Communication). This backflooding induces sinkhole flooding and large intermittent springs upstream the city, which contribute to the flood.

Figure 5 : Inverse flow recorded in a Roman well and a sinkhole during 9th September event, due to backflooding (© G. Jouanen, Association Fontaine de Nîmes)

With a catchment area of 55 km² and a maximum estimated discharge of 30 m³ s⁻¹ in 1988, the specific maximum outflow discharge q_M is equal to 0.55 m³ s⁻¹ km⁻², one of the highest compared to other karst springs studied by Bonacci (2001) in Croatia, France, USA and Yugoslavia. The limited discharge capacity of FdN spring is coherent with a previous analysis (Bonacci, 2001) which considers that karst springs with $q_M < 1$ can be classified as those with limited discharge capacity.

3.3. Saturation of the fissured karst system

Groundwater table has been monitored during the event thanks to a network of water level recorders located in observation wells. The evolution of water levels (Figure 6) shows that the fissured system (out of karst conduits – Mas de Ponge and Mas de Provence wells) has been saturated on 6th and 7th September a few hours after the first event: rate of groundwater rising ranges between 0.2 and 0.5 m h⁻¹. The small fissures are quickly filled by groundwater. During the second event, the infiltrated water could not be stored in the karst and therefore contributed to the surface runoff. Local flooding effects are also observed where geomorphology is favourable, in local depressions for example (flooding at Mas de Provence well in Figure 6). The fast saturation of the fissured karst is due to its small storage capacity partly explained by the little thickness (1 – 10 meters) of the unsaturated zone as shown by small water table depths in wells before the event.

Figure 6 : Water levels evolution in boreholes located in the fissured part of the karst (FK) and karst conduits (KC) during and after the event

This saturation of the fissured karst system induces many intermittent springs located in the whole karst basin. It appears that these springs were discharging and the fissured karst was saturated while the water level in the conduits network was much deeper (Poubelle well in Figure 6). This means that, in this case, the fissures are not saturated by water from the karst conduits as observed in other cases by hydraulic inversion (Marina Bay, Bonacci et al., 2006) but by water infiltrating directly on its shallow part characterized by extreme fracturing, the epikarst. Geochemical information makes it possible to consolidate these interpretations. Indeed, the analysis of the geochemistry of water in the streams during the first flood event (Maréchal and Ladouche, 2006) allows to show, on the basis of isotopic signature ($\delta^{18}\text{O}$ and $^{87}\text{Sr}/^{86}\text{Sr}$) of water, that the water in the stream during the event is composed of event water and not pre-event water (Figure 7). The $\delta^{18}\text{O}$ values of the rainfall event ranges from -5.6 ‰ to -8.3 ‰ (Figure 7a). Owing to the wide temporal variation of isotopic contents in rainfall, the selection of appropriate isotopic composition of event water has been performed using the cumulative incremental weighted approach based on rainfall amount as recommended by McDonnell et al. (1990). The calculated event water isotopic composition fluctuate from -7.2 ‰ to -7.1 ‰ (Figure 7b). The event signature was significantly enriched in ¹⁸O compared to pre-event signature (-7.5 ‰) and allow to explain the temporal signature measured in surface streams during the first flood event.

Figure 7 : (a) Temporal $\delta^{18}\text{O}$ evolution in rainwater, stream water and FdN spring during September events. (b) Representative bi-variate plot showing the pre-event (conduits network characterized at FdN spring), event water [first part (i. e. rainfall of 154 mm) of the first rainfall event (rainfall of 205 mm)] and stream water (Ales and Uzes Cadereaux) during the September 2005 storm flow event

The $^{87}\text{Sr}/^{86}\text{Sr}$ ratios and Sr content of stream water is explained as the result of a mixing between rainwater and Hauterivian groundwater End Members (Figure 8), the rainfall contribution being close to 80 % at the beginning and evaluate to 40 % during the recession of the first flood event only a few hours after the peak. These results suggest that a part of the stream water had an underground travel through the karst (most probably the epikarst), this phenomena allowing to explain the large content in chloride (up to 20 mg/l), nitrate (up to 25 mg/l) and bore (up to 70 $\mu\text{g/l}$) measured in surface waters during the flood event. After the flooding event, the water levels in the boreholes decrease very slowly: recessions are very long due to the bad connection of these parts of the karst with the drainage system. On the contrary, water level decreases quickly in the karst conduits (example of Poubelle well in Figure 6) well connected to the spring of the system.

Figure 8 : $^{87}\text{Sr}/^{86}\text{Sr}$ ratios versus Sr concentration in surface water during the September 2005 storm flow event. The rainwater End Member are defined on the base of bibliographic data, the lower Hauterivian End Member (n3a) and the upper Hauterivian End Member (n3b) have been characterized by springs. The upper Hauterivian (n3b) is well represented in Ales watershed. The lower Hauterivian (n3a) is largely represented in Uzes catchment's. Rainfall contribution is reported on the theoretical mixing lines.

4. Warning system and management

The important role of karst groundwater in the genesis of flood necessitates taking into account that component in the warning system of the Nîmes Municipality; this system being up to now based essentially on monitoring of surface flood using limnimeters and video cameras, and rainfall using rain gauges and radars (Delrieu et al., 1988; Delrieu et al., 2004). The water table will require regular monitoring as an indicator of aquifer saturation during flood crisis. Given that two kinds of dynamics exist in the karst system, two monitoring sites have been proposed:

- One at the spring in order to have information on the state of the whole system and on the conduits saturation level. The water level corresponding to $13 \text{ m}^3 \text{ s}^{-1}$ at the spring, beyond which the backflooding and sinkhole flooding appears in the karst conduits has been proposed as critical threshold;
- One in the fissured aquifer in the vicinity of intermittent springs zone (Figure 1) in order to integrate the long recession period of such part of the system. Threshold has to be determined after a monitoring period.

In addition, modelling of the karst response to rainy events has been used in order to propose meteorological alert thresholds to the city services, beyond which a risk of fissured karst overflowing is present. Flash flood warnings are usually defined as the volume of rain of a given duration necessary to cause flooding (Carpenter et al., 1999). In this study, the threshold is defined as the amount of rain of a given duration able to cause a saturation of the fissured part of karst and therefore increase the risk of flooding. The water level at Mas de Provence well (Figures 1 and 6) has been simulated using an inverse modelling approach based on transfer functions determination (Pinault et al., 2004). Data processing is done using the Tempo tool which is a software for the treatment and modelling of time series in hydrology and hydrochemistry (Pinault et al., 2001). Contrary to the direct modelling, which consists in reproducing the behaviour of a hydrosystem from concepts resting at the same time on the description of this hydrosystem and the application of physics laws, inverse modelling deduces system functioning from the analysis of data. The causal relationship between inputs and output

of the system is materialized by one or more transfer functions describing the various processes: runoff, infiltration, and groundwater flow. When several independent impulse responses are required to modelling, the system is known as non-linear. Using Potential Evapo-Transpiration and rainfall time series observed at local meteorological stations as input, the model allows determining transfer functions able to reproduce the observed output time series (i.e. water level time series observed at Mas de Provence well in this case, Figure 9). Thus, (1) the input of the system is defined as the quantity of rain which will induce a water level variation, considering that a part of the rain is lost out of the system. (2) A threshold (Ω), variable with time, separates the actual rainfall (R) from the lost one by evapo-transpiration. (3) The impulse responses of the outflow (Γ) to effective rainfall are then computed through an iteration process.

Figure 9: Basic structure of the transfer model

The best adjustment of observed data has been obtained using two impulse responses (Figure 10b): one quick impulse response (mean transit time: 2 days) and one slow impulse response (mean transit time: 22 days). Comparison of observed and simulated water table during the calibration period shows that the model is globally satisfying with a Nash coefficient equal to 0.86 (Figure 10a). Effective rainfall is 54.8 % of total rainfall. The timing of both overflowing events of November 2004 and September 2005 is correctly simulated. An overestimation of water table during the latest is nevertheless observed. During these events, two lacks of observation data are due to the overflowing karst (water table in the observation well has reached the top of the well and the monitoring system has been flooded). If the water table is not perfectly simulated during high floods, the model correctly simulates occurrence of karst overflow during high rainfall events and absence of overflow during medium rainfall events or low flow condition. This allows its use for the determination of a rainfall threshold for karst overflowing.

Figure 10: Inverse modelling of the Mas de Provence well. Sampling rate is 1 day. (a) Comparison between modelled and observed levels. The Nash coefficient is 0.86 (b) Impulse responses of the Mas de Provence well to rainfall (July 2004 – December 2005).

Using the defined transfer functions, it is possible to simulate the water table during the last 7 years and compare it to the rainfall data (Figure 11). This comparison allows defining by a series of attempts a well suited rainfall threshold able to identify the periods of karst overflowing. On Figure 11, the cumulative rainfall computed on 25 days gave a satisfying result with a threshold at 145 mm. This long duration, close to the mean transit time of slow impulse response is due to the long recession in the low permeable part of the karst as observed at Mas de Provence well on Figure 11b. This promising approach must be applied on several wells in order to consider the spatial variability of karst response according to hydrodynamic properties and water table depth.

Figure 11: (a) Cumulative rainfall observed during 25 days from 1999 and rainfall threshold at 145 mm (b) Simulation of water table from 1999 and warning system considering a 25 days - cumulative rainfall threshold at 145 mm

5. Conclusion

The extensive monitoring of the September 2005 event shows that the Nîmes karst system is characterized by karst flash flooding. Analysis of November 2004 event leads to the same conclusion.

The specific characteristics of the Nîmes karst favouring karst-flash-flood are: (i) high infiltration rate due to scarce and highly permeable soils; (ii) rapid infiltration of storm flow entering the aquifer quickly through sinkhole drains, (iii) rapid circulation in well developed karstic conduits network; (iv) backflooding and sinkhole flooding close to the spring due to conduit constriction and (v) small storage capacity of fissured karst system and therefore infiltration excess runoff genesis.

The contribution of groundwater must then be considered as a possible aggravating factor in flash flood genesis. A methodology comprising modelling of the karst system allowed proposing a simple meteorological threshold for fissured karst overflowing.

Acknowledgments

This research has been conducted thanks to the collaboration and the funding of Nîmes Municipality and French Minister of the Environment and Sustainable Development.

References

Andreo B, Goldscheider N, Vadillo I, Vias JM, Neukum C, Sinreich M, Jimenez P, Brechenmacher J, Carrasco F, Hotzl H, Perles MJ, and Zwahlen F., 2006. Karst groundwater protection: First application of a Pan-European Approach to vulnerability, hazard and risk mapping in the Sierra de Libar (Southern Spain). *Science of the Total Environment*, 357(1-3): 54-73.

Atkinson, T. C., 1977. Diffuse flow and conduit flow in limestone terrain in Mendip Hills, Somerset (Great Britain), *J. Hydrol.*, 35, 93–100.

Ballais, J.L., Garry, G. and Masson, M., 2005. Contribution of hydrogeomorphological method to flood hazard assessment: the case of French Mediterranean region. *C.R. Geoscience*, 337, 1120-1130.

Bonacci, O., 2001. Analysis of the maximum discharge of karst springs. *Hydrogeology Journal*, 9, 328-338.

Bonacci, O., Ljubenkovic, I. and Roje-Bonacci, T., 2006. Karst flash floods: an example from the Dinaric karst (Croatia). *Nat. Hazards Earth Syst. Sci.*, 6: 195-203.

Carpenter, T.M., Sperflage, J.A., Georgakakos, K.P., Sweeney, T. and Fread, D.L. 1999. National threshold runoff estimation utilizing GIS in support of operational flash flood warning systems. *Journal of Hydrology*, 224, 21-44.

Delrieu G., A. Bellon, and J.D. Creutin, 1988. Estimation de lames d'eau spatiales à l'aide de données de pluviomètres et de radar météorologique (Rainfall estimation using rain gauge and radar data). *Journal of Hydrology*, 98, 315-344.

Delrieu, G., Andrieu, H., Anquetin, S., Creutin, J.D., Ducrocq, V., Gaume, E. and Nicol, J., 2004. Cevennes-Vivarais Mediterranean hydro-meteorological observatory: the catastrophic rain event of 8-9 September 2002 in the Gard region, France. *Sixth International Symposium on Hydrological Applications of Weather Radar*, Melbourne, Australia, 2-4 February 2004.

Fabre, G., 1990. La catastrophe hydrologique éclairée de Nîmes (3 octobre 1988). The Nîmes flash flood on October 3, 1988. *Bulletin de l'Association de Géographes Français*, 67(2): 113-122.

Fabre, G., 1997. Le bassin d'alimentation de la fontaine de Nîmes d'après les expériences de traçages. *Bul. Soc. et Sc. Nat. Nîmes et Gard*, 61: 52-57.

Fabre, G. and Guyot, J.L., 1984. Première série continue de jaugeages sur la Fontaine de Nîmes (Gard); données et interprétations des principaux résultats. Gauging the Nîmes Spring (Gara); data and interpretation of initial results. *Travaux*, 13: 65-78.

Fabre, G. and Guyot, J.L., 1988. Sur l'hydrologie karstique de la Fontaine de Nîmes (Gard). Karst hydrology of Nîmes Fountain, Gard. *Bulletin de la Société d'Etude des Sciences Naturelles de Nîmes*, 58: 39-47.

Gaume, E., Livet, M., Desbordes, M. and Villeneuve, J.P., 2004. Hydrological analysis of the river Aude, France, flash flood on 12 and 13 November 1999. *J. Hydrol.* 286, 135-154.

Georgakakos, K.P., 1986. On the design of national, real-time warning systems with capability for site-specific, flash-flood forecasts. *Bulletin of the American Meteorological Society* 67(10): 1233-1239.

Kaufmann, O. and Quinif, Y., 1999. Cover-collapse sinkholes in the "Tournaisis" area, southern Belgium; Sinkholes and the engineering and environmental impacts of karst. Sixth multidisciplinary conference on Sinkholes and the engineering and environmental impacts of karst, Springfield, MO, United States, 1997 - *Engineering Geology*, 52(1-2): 15-22.

Kiraly, L., 1994. Groundwater flow in fractures rocks: models and reality, 14th Mintrop Seminar "über Interpretationsstrategien in Exploration und Produktion, Ruhr Universität" at Bochum, 159, 1-21.

Lolcama, J.L., Cohen, H.A. and Tonkin, M.J., 2002. Deep karst conduits, flooding, and sinkholes; lessons for the aggregates industry; Engineering and environmental impacts of karst. Seventh multidisciplinary conference on Sinkholes and the engineering and environmental impacts of karst, Harrisburg, PA, United States, Apr. 10-14, 1999 - *Engineering Geology*, 65(2-3): 151-157.

Lowe, D. and Waltham, T., 2002. Dictionary of karst and caves; a brief guide to the terminology and concepts of cave and karst science. *BCRA Cave Studies Series*, 10: 40.

Maréchal, J.C., Ladouche, B., Courtois, N. and Dörfliger, N. 2005. Modèle conceptuel de la structure et du fonctionnement du système karstique de la Fontaine de Nîmes. BRGM/RP-53827-FR, BRGM, 187 p.

Maréchal, J.C. and Ladouche, B., 2006. Fonctionnement hydrogéologique du système karstique de la Fontaine de Nîmes en crue, Rapport final, BRGM/RP-54723-FR, BRGM, 111 p.

McDonnell, J. J., Bonell, M., Stewart, M. K. and Pearce, A. J. 1990. Deuterium variations in storm rainfall : implications for stream hydrograph separation. *Water Resources Research*, 26(3): 455-458

O'Connor, P.J., Gallagher, V., Madden, J.S., Van den Boom, G., McLaughlin, J.P., McAulay, I.R., Barton, K.J., Duffy, J.T., Muller, R., Grimley, S., Marsh, D., Mackin, G. & Mac Niocaill, C. 1993. Assessment of the geological factors influencing the occurrence of radon hazard areas in a karstic region, Geological Survey of Ireland Report Series, 93/2, 204 p.

Pinault, J.L., 2001. Manuel utilisateur de TEMPO: Logiciel de traitement et de modélisation des séries temporelles en hydrogéologie et en hydrogéochimie. *Projet Modhydro*. BRGM/RP-51459-FR, BRGM.

Pinault, J.L., Doerfliger, N., Ladouche, B. and Bakalowicz, M., 2004. Characterizing a coastal karst aquifer using an inverse modeling approach; the saline springs of Thau, southern France. *Water Resources Research*, 40(8): 17.

Pinault, J.L., Plagnes, V., Aquilina, L. and Bakalowicz, M., 2001. Inverse modeling of the hydrological and the hydrochemical behavior of hydrosystems: Characterization of karst system functioning. *Water Resources Research*, 37(8): 2191-2204.

Raymond, M., Peyron, N. and Martin, A. 2006. ESPADA, A unique flood management tool: first feedback from the September 2005 flood in Nîmes. 7th International Conference on Hydroinformatics, HIC 2006, Nice, France.

Smith, K. and Ward, R., 1998. *Floods – physical processes and human impacts*, John Wiley and Sons, Chichester.

Stanescu, V.A., Matreata, M., 1997. Large floods in Europe. In: *Proc Flow Regimes from International Experimental and Network Data*, 3rd Rep, UNESCO, Cemagref, Paris, 229–236.

Figures

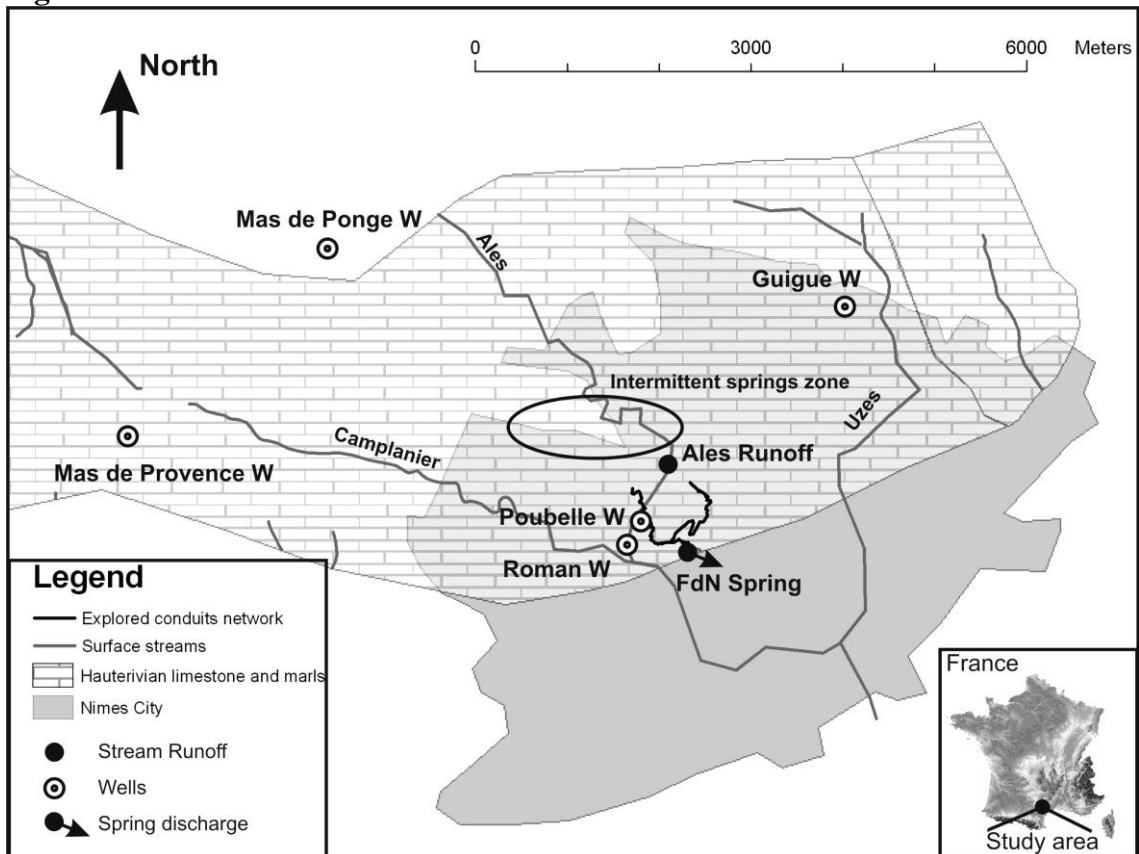


Figure 1: location of the Eastern part of Nîmes karst system and Nîmes city area. Location of monitoring network.

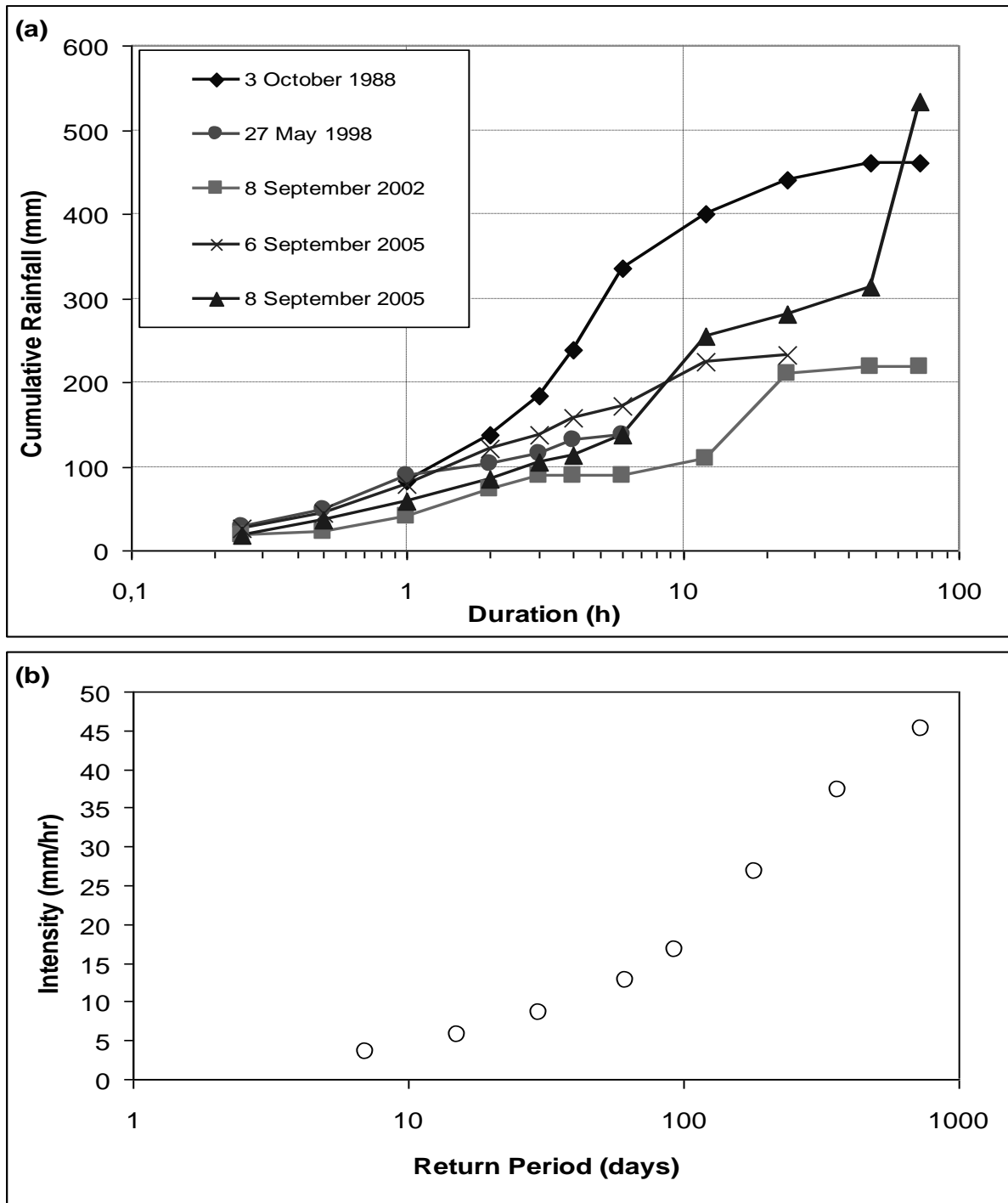


Figure 2 : (a) cumulative rainfall according to duration of the last main rainfall events at Nîmes (after Raymond et al., 2006); (b) Return period of rainfall of one hour duration at Nîmes Courbessac meteorological station

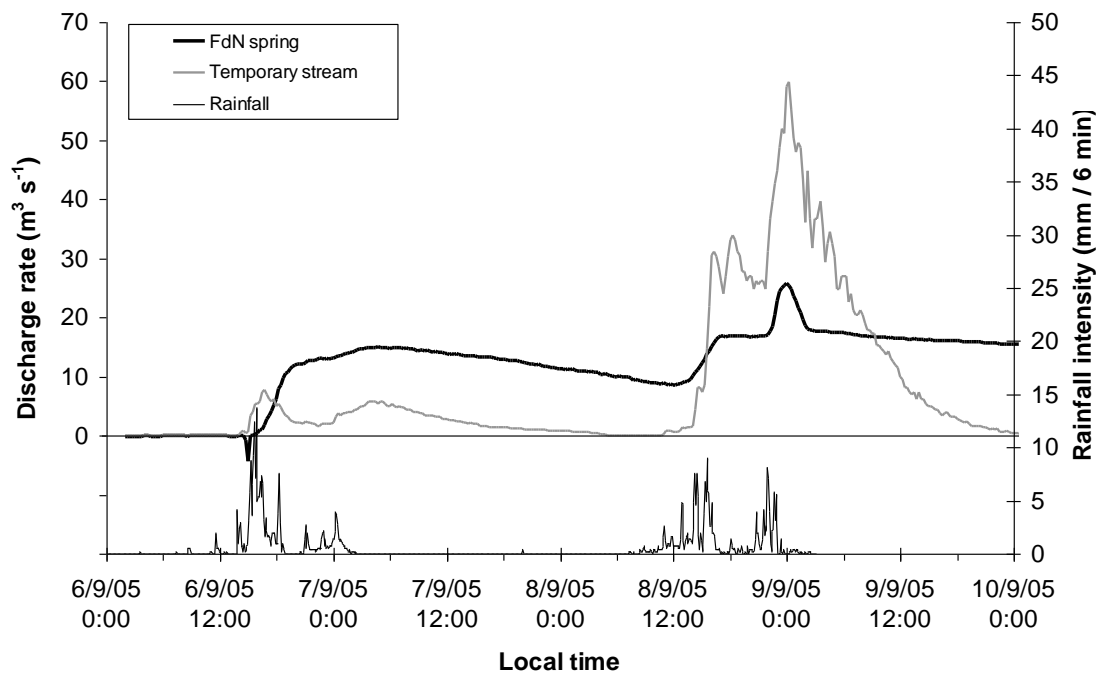


Figure 3: Discharge rate of the main spring of the karst system (FdN spring) and in a surface stream during September 2005 event

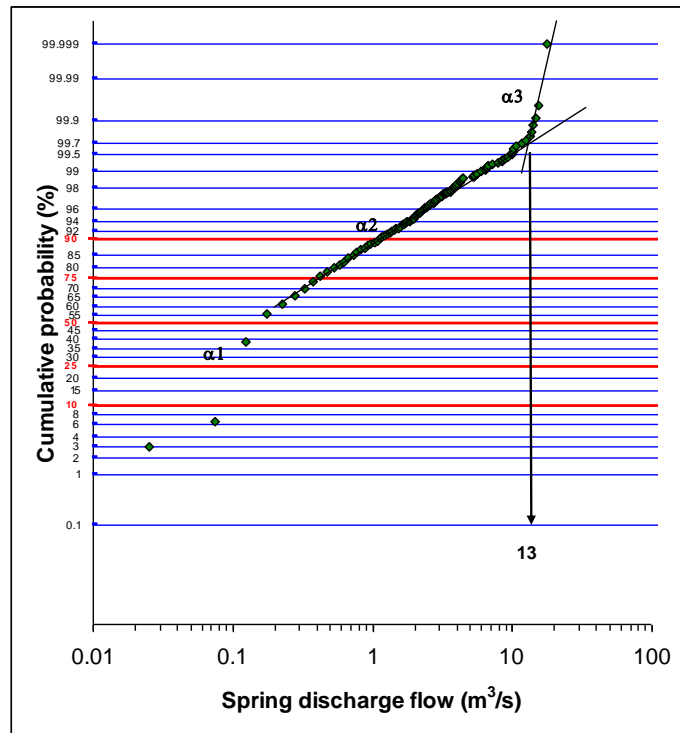


Figure 4: Sorted discharge rates of FdN spring during 1998-2005 period (0.05 m³/s class)

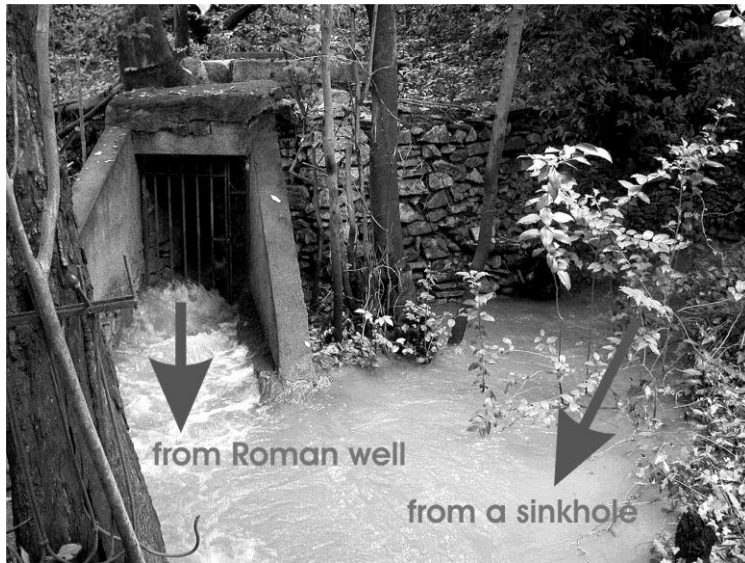


Figure 5: Inverse flow recorded in a Roman well and a sinkhole during 9th September event, due to backflooding (© G. Jouanen, Association Fontaine de Nîmes)

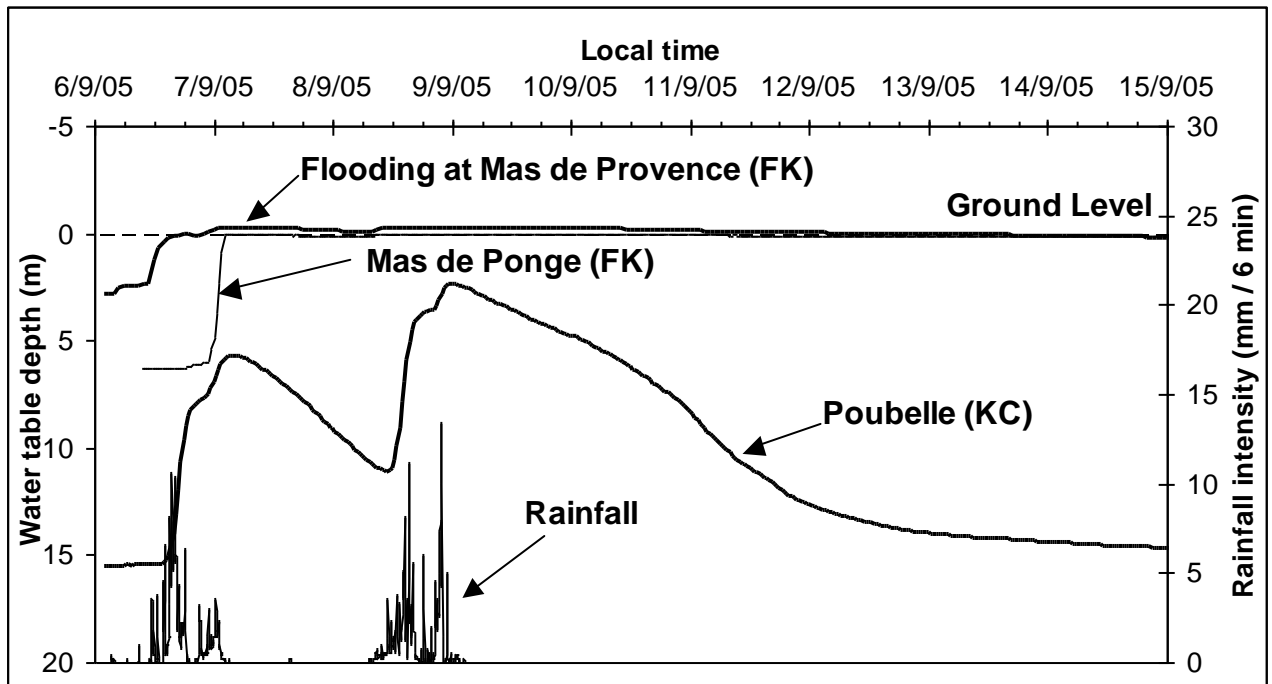


Figure 6: Water levels evolution in boreholes located in the fissured part of the karst (FK) and karst conduits (KC) during and after the event. Location of boreholes is shown in Figure 1.

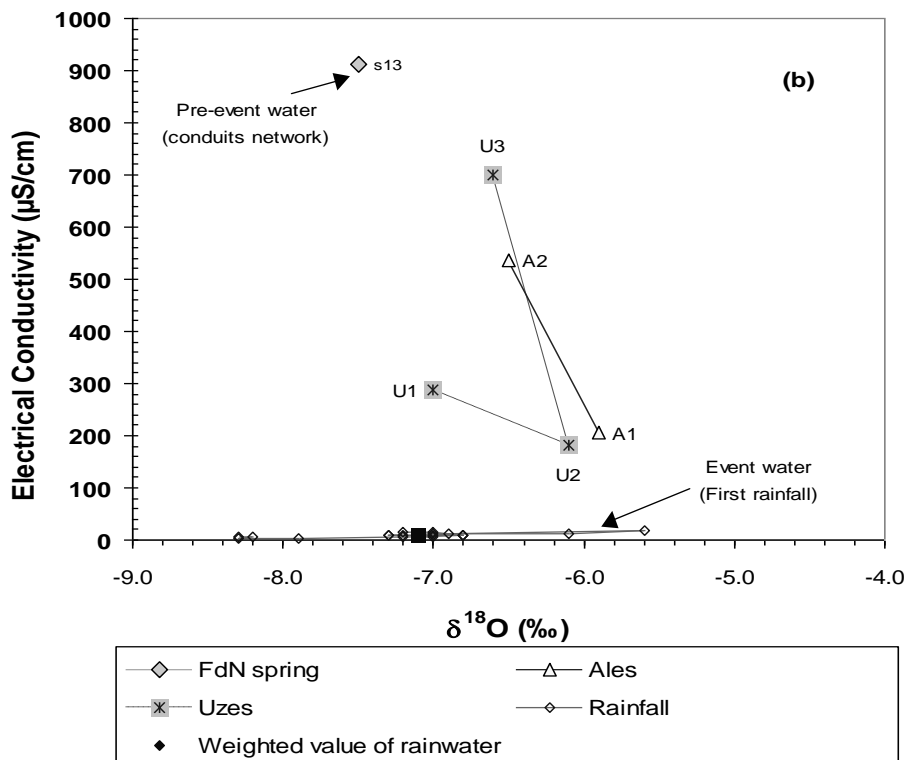
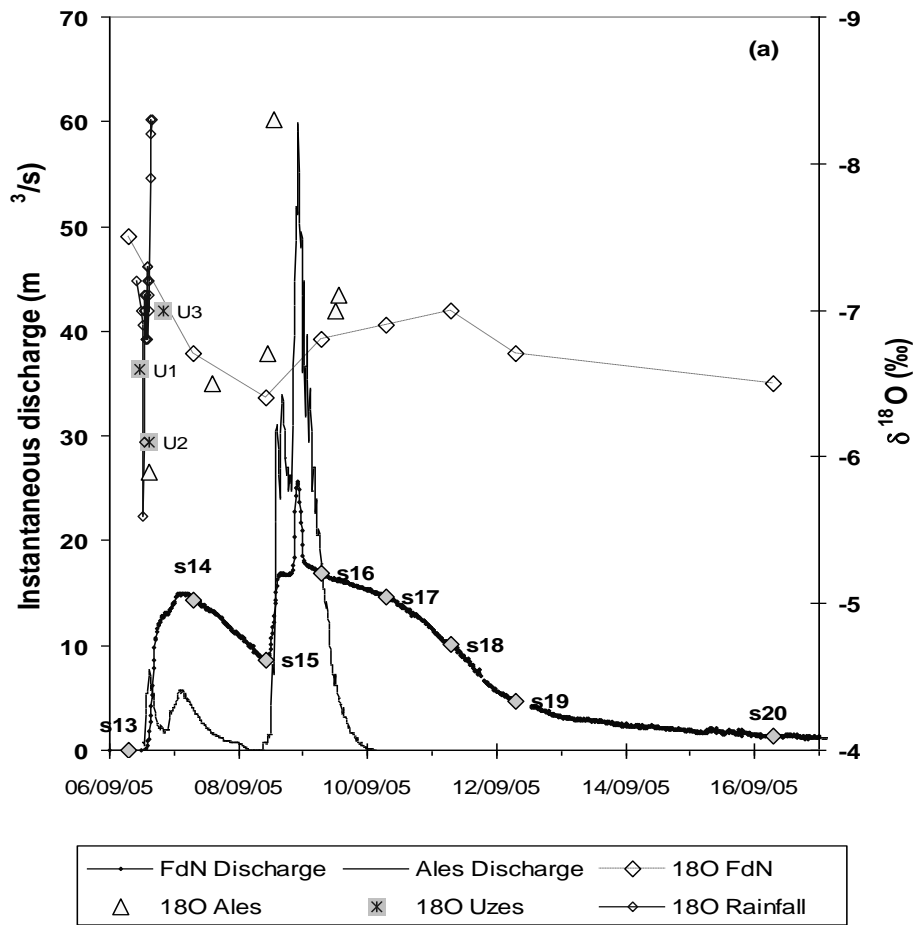


Figure 7: (a) Temporal $\delta^{18}\text{O}$ evolution in rainwater, stream water and FdN spring during September events. (b) Representative plot showing the pre-event (conduits network characterized at FdN spring), event water [first part (i. e. rainfall of 154 mm) of the first rainfall event (rainfall of 205 mm)] and stream water (Ales and Uzes Cadereaux) during the September 2005 storm flow event

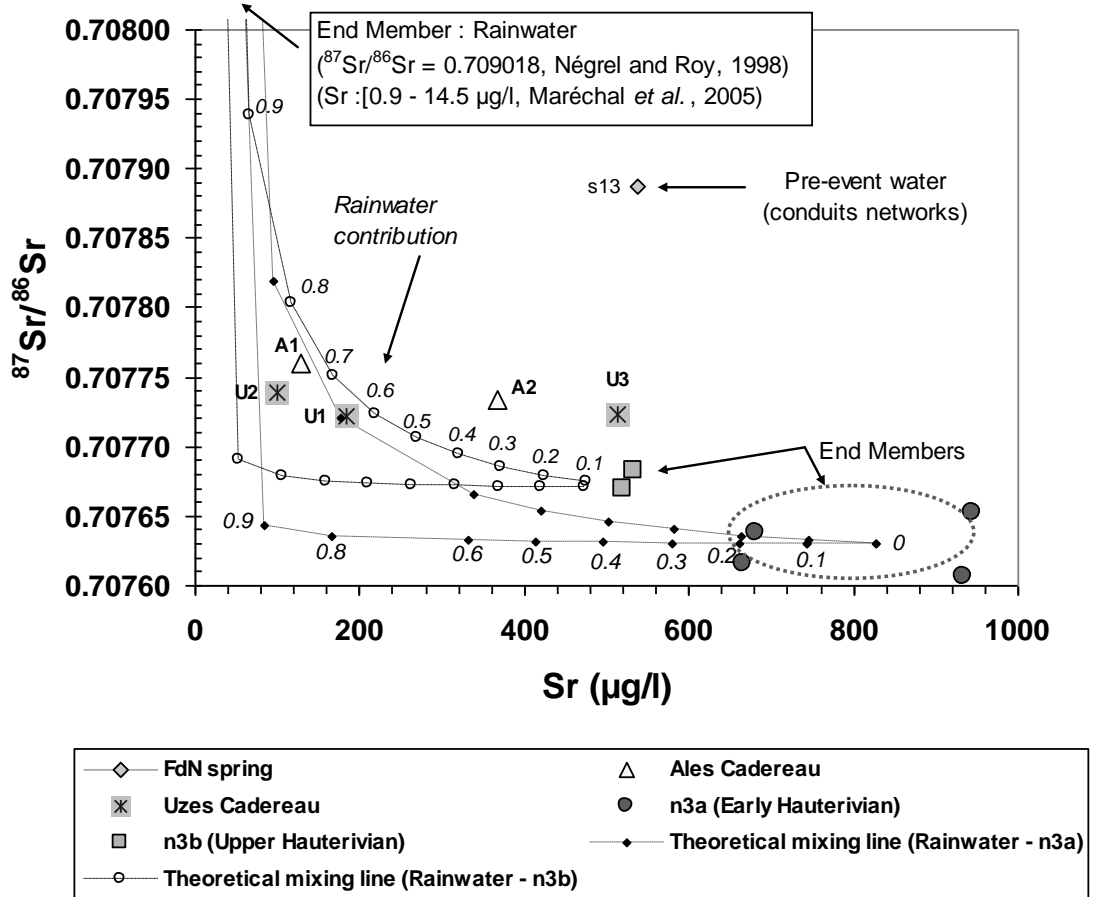


Figure 8: $^{87}\text{Sr}/^{86}\text{Sr}$ ratios versus Sr concentration in surface water during the September 2005 storm flow event. The rainwater End Member are defined on the base of bibliographic data, the lower Hauterivian End Member (n3a) and the upper Hauterivian End Member (n3b) have been characterized by springs. The upper Hauterivian (n3b) is well represented in Ales watershed. The lower Hauterivian (n3a) is largely represented in Uzes catchment's. Rainfall contribution is reported on the theoretical mixing lines.

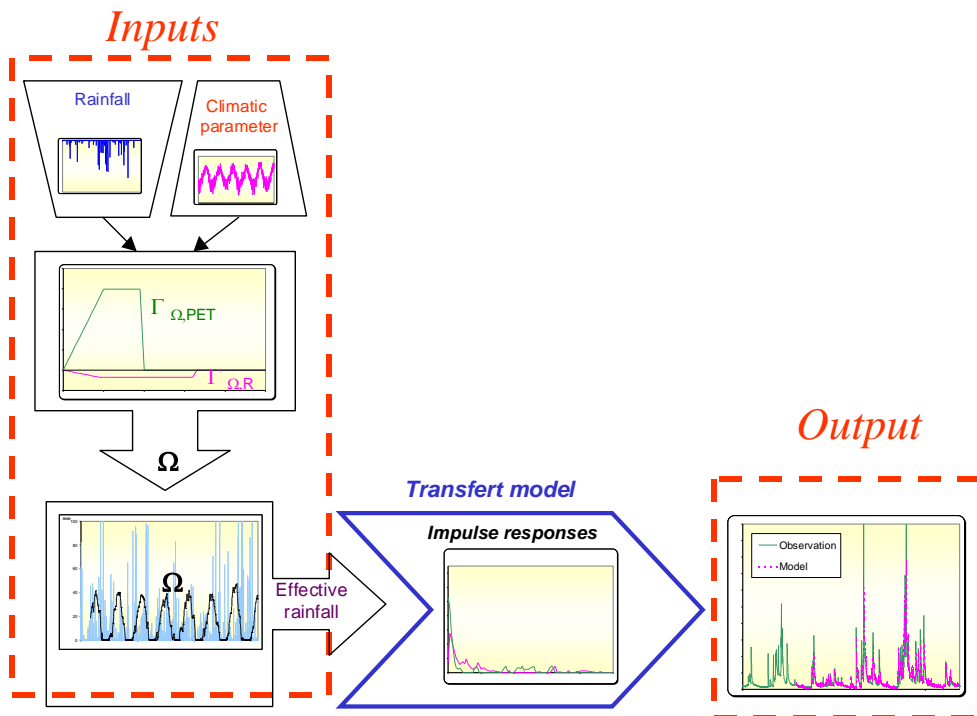


Figure 9: One type of the basic structure of the transfer model

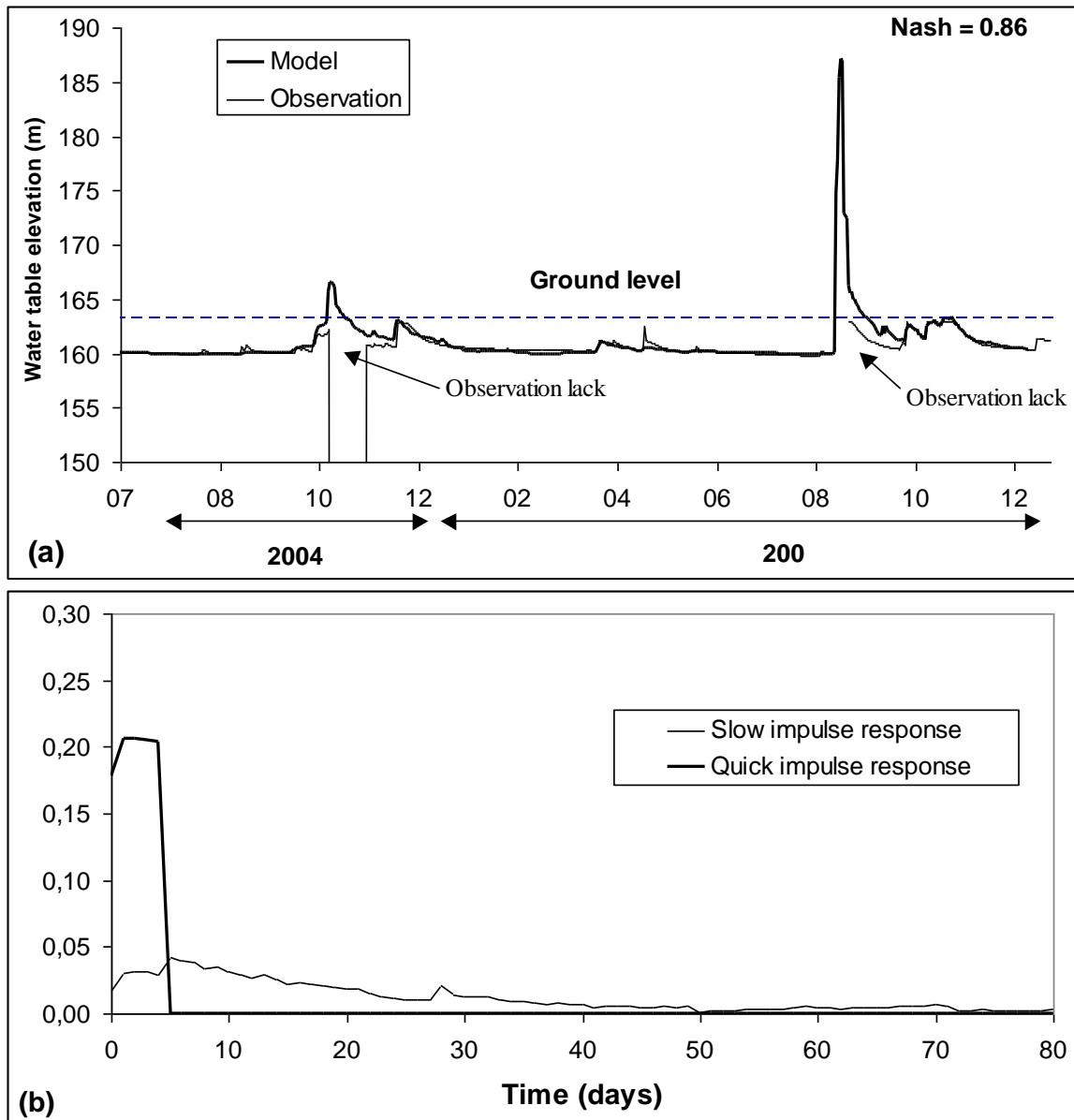


Figure 10: Inverse modelling of the Mas de Provence well. Sampling rate is 1 day. (a) Comparison between modelled and observed levels. The Nash coefficient is 0.86 (b) Impulse responses of the Mas de Provence well to rainfall (July 2004 – December 2005).

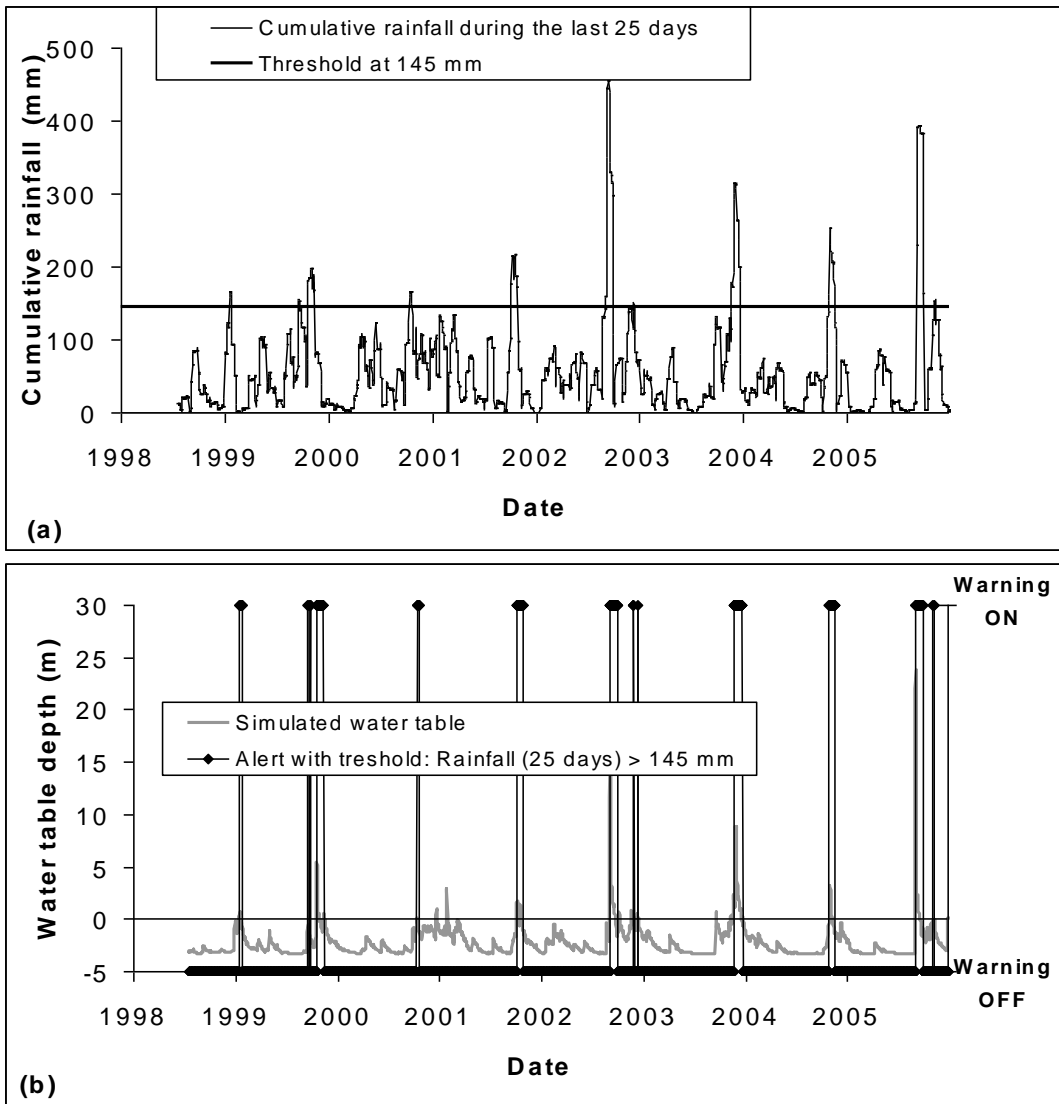


Figure 11: (a) Cumulative rainfall observed during 25 days from 1999 and rainfall threshold at 145 mm (b) Simulation of water table from 1999 and warning system considering a 25 days - cumulative rainfall threshold at 145 mm